International Journal of Pharmaceutics 409 (2011) 1–8

Contents lists available at ScienceDirect

International Journal of Pharmaceutics

journal homepage: www.elsevier.com/locate/ijpharm

Hollow porous implants filled with mesoporous silica particles as a two-stage antibiotic-eluting device

Luis Manuel Perez[a,1], Patricia Lalueza[a,1], Marta Monzon[b], José Antonio Puertolas[c], Manuel Arruebo[a,*], Jesús Santamaría[a,d,*]

[a] Aragon Nanoscience Institute (INA), C/Mariano Esquillor, Edif. I + D, University of Zaragoza, 50018 Zaragoza, Spain
[b] Department of Animal Pathology, Veterinary School, University of Zaragoza, 50013 Zaragoza, Spain
[c] Department of Materials Science and Technology, CPS-I3A, Maria de Luna 3, University of Zaragoza, 50018 Zaragoza, Spain
[d] CIBER de Bioingeniería, Biomateriales y Nanomedicina, CIBER-BBN, Spain

ARTICLE INFO

Article history:
Received 6 October 2010
Received in revised form 8 February 2011
Accepted 9 February 2011
Available online 16 February 2011

Keywords:
Hollow prosthesis
Controlled release
Infection
Orthopedic surgery
Traumatology
Staphylococcus aureus
Mesoporous silica
Linezolid

ABSTRACT

A new type of implantable drug eluting device is presented, consisting of a bed of mesoporous microparticles packed inside a reservoir with a porous wall. This provides two sets of variables for drug release control that can be tailored independently. The first is related to the microparticles (packing density, size and pore structure) and the second to the reservoir (pore diameter and thickness of the wall, permeation area). In this work the concept is developed into a working model, used to fight bacterial (*Staphylococcus aureus*) growth by releasing linezolid that had previously been adsorbed on silica microparticles. These particles were placed inside the hollow interior of a porous medical grade stainless steel pin mimicking those used in traumatology and in orthopedic surgery. The mechanical behavior of the porous drug-eluting pin was tested and found satisfactory.

© 2011 Elsevier B.V. All rights reserved.

1. Introduction

Despite the advances achieved in orthopedic surgery, sterility levels in operating rooms, and developments in parenteral antibiotic prophylaxis, bacterial infections continue to be a major complication after implantation. Infection of bones (osteomyelitis) and joints (septic arthritis) without prompt treatment can become chronic when bacterial biofilm is not completely eradicated. When biofilm is formed, a systemic treatment with antibiotics is needed often accompanied by surgical alternatives including debridement and prosthesis retention; re-implantation with either a single- or two-stage exchange arthroplasty (shoulder, hip) or arthrodesis (knee) (Bernard et al., 2004). There is general agreement that for hip surgery, an infection rate of less than 1% should be achievable; for other joints the rate is higher because of their proximity to the skin surface and a more limited experience in joint design (Lew and Waldvogel, 2004). In this way, open fractures are frequently accompanied by bacterial contamination. In some of those cases fixation devices either external (i.e., Illizarov frames, Schanz pins, etc.) or internal (intramedullar nails, plates, etc.) are used for stabilization of the healing bone. Those orthopedic external fixation devices used for traumatology or for reconstruction are placed externally from the body but connected to the bone through pins. The connection across skin and tissue can be a critical entry point for bacterial invasion. Usually, daily pin care is performed, involving cleansing of the pin/skin interface with isopropyl alcohol and removing any crusted, weeping edema fluid. This generally provides adequate care (Bibbo and Brueggeman, 2010), although recalcitrant non-healing pin sites still occur, together with pin-site infections (Mason et al., 2005). Therefore, both traumatology and orthopedic surgery may potentially benefit from the use of on-site drug-eluting devices and scaffolds that help to prevent bacterial infection providing local concentrations of an antibiotic at least above the minimal inhibitory concentration (MIC) but below the systemic toxicological threshold.

Due to the poor bone vascularization the local concentration that can be reached with systemically applied antibiotics in the bone is low; to solve this drawback, local antibiotic release from polymethyl methacrylate (PMMA)-based bone cements was already postulated in the 70s (Buchholz and Engelbrecht, 1970). Despite their success (Engesaeter et al., 2003) an important disad-

* Corresponding authors. Tel.: +34 976761000x3514; fax: +34 976762142.
E-mail address: arruebom@unizar.es (M. Arruebo).
[1] Both authors contributed equally to the work.

0378-5173/$ – see front matter © 2011 Elsevier B.V. All rights reserved.
doi:10.1016/j.ijpharm.2011.02.015

vantage of using antibiotic-loaded PMMA beads is that a second surgery is necessary to remove them. Also, antibiotic loaded bone cements cannot be used when hydroxyapatite coated prostheses are employed (Laurent et al., 2008). Most of the alternatives to solve the deficiencies of acrylic bone cements explore their replacement by drug-eluting biodegradable materials that act as scaffolds and will not require surgical removal when added, either as monolithic structures or as microparticulate materials (Arruebo et al., 2010).

Hence, some materials act as re-sorbable scaffolds for bone regeneration, others act as fixation systems which are temporarily or permanently located in the bone until healing and both scenarios are prone to bacterial infection. The design of scaffolds or prosthesis with antibiotic eluting characteristics is therefore interesting in the broad fields of traumatology and orthopedic surgery.

Many medical devices with drug-eluting properties have been designed (Arruebo et al., 2010). Among the examples, porous titanium-based implants have been used *in vitro* as growth-factor delivery vehicles (Clark et al., 2008). Ceramic blocks of antibiotic impregnated calcium hydroxyapatite have been implanted in patients who received resection arthroplasty, demonstrating no evidence of a recurrent infection in the 86% of them (Sudo et al., 2008). In order to control the diffusion kinetics of a previously encapsulated drug, top–down microfabrication techniques were used to create silicon-based membranes that were used as release windows on drug reservoirs formed from a cylindrical titanium alloy hollow enclosure (Martin et al., 2005). On the other hand, porous ceramic matrices including calcium phosphates (Yu et al., 1992) and ordered silica mesoporous materials are well known as porous materials capable of adsorbing and releasing drugs on a controlled manner (Vallet-Regi, 2006), although they have not been used to build prosthetic devices, probably because self-supported structures formed by these materials alone lack mechanical stability. This problem is partly solved when composite materials are used as scaffolds for bone regeneration since they combine the mechanical properties of biodegradable polymeric materials with the ability to control the release obtained with inorganic mesoporous materials. However, when high mechanical resistance and fixation capabilities are needed to support a healing bone, structures formed of metals such as medical grade CoCrMo, Ti6Al4V or 316L stainless steel are commonly used.

In this work we present a drug releasing device in which the drug release rate is controlled by coupling two mass-transport stages in series. In a first stage, the drug adsorbed on a packed bed of microparticles is released into the inner space of a drug reservoir. The second step corresponds to the permeation of the desorbed drug through the porous wall of the reservoir, constituted by a porous membrane of suitable permeation characteristics. The concept is schematically shown in Fig. 1. As a proof of concept we designed a porous 316L stainless steel reservoir that mimics the pins used in external frame fracture fixation. We loaded its hollow interior with mesoporous silica microparticles in whose pores an antibiotic had previously been adsorbed and studied the release to the fluid surrounding the reservoir. The mechanical performance of this porous stainless steel has also been assessed.

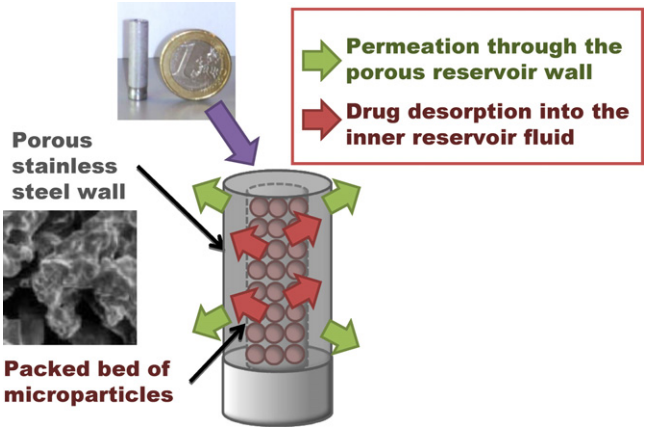

Fig. 1. Conceptual scheme of the drug release device.

2. Materials and methods

2.1. Materials synthesis and drug loading

Spherical mesoporous microparticles (~440 nm) with the MCM-48 cubic structure were synthesized according to the procedure previously described (Pérez et al., 2007) but reducing the amount of silica precursor (TEOS) used. These microparticles were characterized by X-Ray diffraction (on Philips X'pert MPD diffractometer with a thin film attachment for low angle glazing incidence measurements), Scanning and Transmission Electron Microscopy (on a SEM Hitachi S2300 and a Tecnai® F30 from FEI® Instruments, respectively) and N_2 adsorption analysis (on a Micromeritics ASAP2010 analyzer). The microparticles were packed inside hollow porous 316L stainless steel pins purchased from Mott Corporation (Farmington, USA). The pins had one open end which was used to load the particles, while a blind end cap was welded on the opposite side. Each pin has a porous length of 25.4 mm and an outside diameter of 6.35 mm with a wall thickness of 1.6 mm (Fig. 1). The nominal filtration cutoff size of the steel is 200 nm and its volumetric porosity of 17%. The inner volume of the hollow pins was packed with drug-loaded mesoporous particles. The material was carefully loaded, with frequent tapping of the tube to have a densely packed bed and ensure packing reproducibility.

Linezolid is a synthetic antibiotic, member of the oxazolidinone class of drugs which has been used to treat a large number of resistant strains of bacteria. For adsorption loading, commercial linezolid (Zyvoxid®) solution (10 mL, 2 mg/mL) was put in contact for 18 h with 100 mg of the MCM-48 spheres at room temperature in an orbital shaker. Previously, the dispersion was sonicated during 5 min to break down agglomerates. Adsorption isotherms were evaluated by measuring the linezolid concentration in the supernatant by using UV–vis spectrophotometry (at 251 nm) at fixed time intervals. To avoid interference in the measurement by suspended silica microparticles, the powder was separated from the supernatant in a centrifuge (10,000 rpm, 20 min) and by filtration (200 nm cut-off). The possible interference in the UV–vis at the frequency used from the other components present in the commercial antibiotic formulation was evaluated and ruled out. Desorption isotherms were evaluated by packing the hollow pins with ~37 mg of linezolid-adsorbed MCM-48 particles and immersing the loaded pins in 50 mL of simulated body fluid (SBF), prepared according to the method described by Kokubo et al., 1990, at 37 °C under stirring. The SBF solution has the following molar concentration: $142Na^+:5K^+:1.5Mg^{2+}:2.5Ca^{2+}:148.8Cl^-:4.2HCO_3^-:1HPO_4^{2-}$ (Kokubo et al., 1990). The thermal stability of the linezolid at 37 °C over time was studied and verified (no absorbance-peak shift was observed after 22 days of analysis and new absorption peaks which could indicate the presence of degradation by-products were not observed either). TGA analysis (Mettler Toledo TGA/SDTA 851e equipment, up to 600 °C under O_2 atmosphere, 1°/min) was performed after drug loading and after drug release, respectively, to quantify the amount of drug loaded on and released from the mesoporous materials.

2.2. Bactericidal studies

Staphylococcus aureus and *epidermidis* are the most common pathogens causing implant-associated infections (Wu et al., 2003). For this reason, the former was chosen in this work. *S. aureus* strain ATCC 29213 was used in all the experiments. For electron-microscopy observation the bacteria samples were fixed with 2 wt.% glutaraldehyde–0.1 M sodium cacodylate buffer supplemented with 4.5 wt.% of sucrose for 1 h 30 min at 37 °C. Bacteria were then dehydrated in a graded methanol series. The samples were sputtered with gold and observed in a Hitachi S-2300 scanning electron microscope.

The linezolid commercial solution was filter-sterilized (pore diameter 200 nm), stored at 4 °C and diluted to the concentration chosen for each experiment. The classical broth microdilution method (Wikler, 2009) was applied to determine the minimal inhibitory concentration (MIC) and the minimal bactericidal concentration (MBC). MBC was defined as a 99.99% reduction of cell viability with respect to that of the initial inoculums.

Pins loaded with linezolid-adsorbed mesoporous silica particles were co-cultured with the *S. aureus* colonies. Previously to the assay, each empty pin was autoclave sterilized, then filled with the drug-loaded microparticles and capped with a PTFE conic plug. The pieces were placed in tubes containing 4 mL of TSB and 100 μL of a stationary culture of the isolate. Bacterial biofilm formation was studied for the pins at 1, 2, 12, 24 or 48 h at 37 °C. Growth medium was discarded and freshly added every 12 h when biofilms of 24 and 48 h were formed. Tests were done in duplicate and a control was included using a pin with no antibiotic. Colonized pins were recovered under sterility and washed with phosphate buffered saline (PBS) to remove unbound bacteria. The average number of bacteria was measured by plate count after sonication at 40 Hz for 15 min (in case of 1, 2 and 12 h biofilms) or 30 min (in case of 24 and 48 h biofilms) at room temperature to disintegrate biofilm cell aggregates.

2.3. Mechanical studies

Tubes of porous stainless steel 316L were purchased from Mott Corporation (Farmington, USA). The tubes had the same porosity, nominal filtration rate, external diameter and wall thickness than the porous pins used in the drug release and bactericidal experiments but different lengths due to the physical requirements of each specific mechanical test.

Uniaxial and unconfined compression tests were performed on porous tubes with 9.5 mm in external diameter, 10 cm long, and a wall thickness of 1.6 mm. Also solid tubing of 316L stainless steel of the same dimensions was purchased to establish a comparison point. The experiments were carried out in an Instrom 8032 testing machine fitted with a 100 kN load cell. The samples were compressed between two steel disks of 20 mm diameter at a crosshead speed of 1 mm/s up to a strain less than 0.5. The porous stainless steel samples were tubes with the same characteristics than the pins but with a length of 10 mm. Five samples were tested and the average and standard error were calculated.

A three point bending test was performed, consisting of a simple supported beam subjected to a point wise central force. The beam corresponded to a tube of stainless steel with a span of 30 mm. The bending test was performed in an Instron 8032 machine with a 100 kN load cell, at a displacement rate of 1 mm/min up to the fracture. Three samples were tested and the average and standard deviation were calculated.

Torsion test were performed up to the final fracture in a set-up machine (Metaltest, Spain) with a torque cell of 100 Nm. Three samples were fractured in this test.

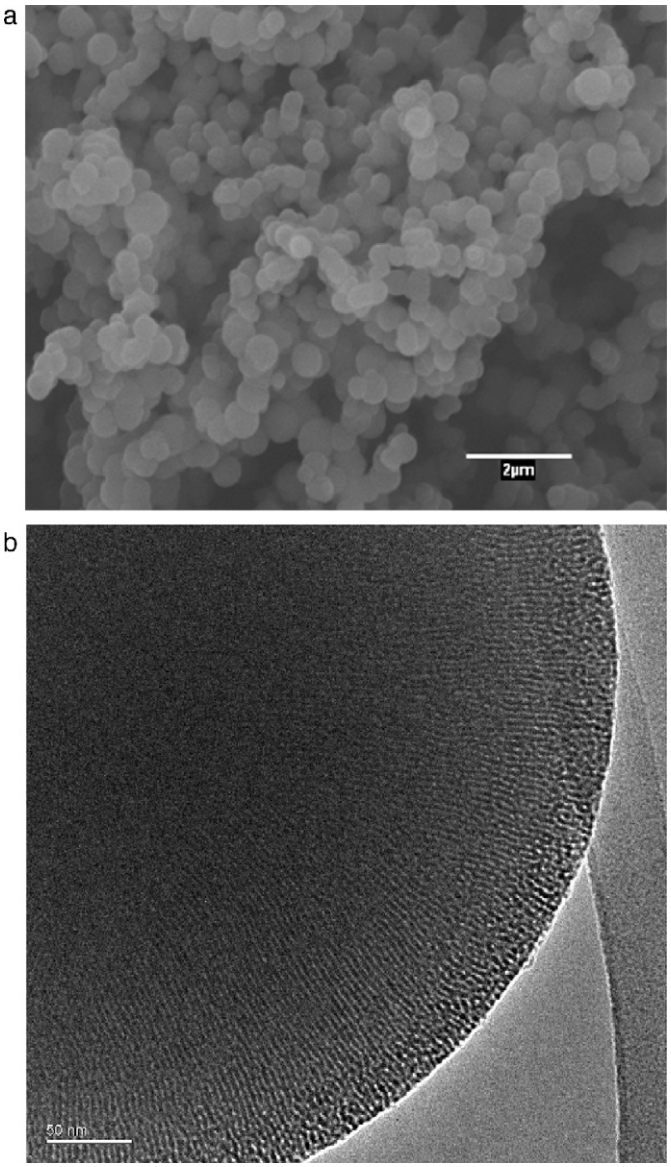

Fig. 2. SEM (A) and TEM (B) views of the silica microparticles used in this work.

3. Results

3.1. Materials synthesis and drug loading

A SEM view of the microparticles used inside the porous-wall reservoir is shown in Fig. 2A. It can be seen that their size is rather homogeneous (~440 nm). Fig. 2B is a TEM view of this material, where the mesoporous structure is observable. Small angle XRD results (not shown) indicated that these microparticles had the MCM-48 structure, with 3-D interconnecting mesopores. N_2 adsorption measurements gave a BET area of 1105.7 m^2/g, with a pore volume of 0.624 cm^3/g and pore sizes of 2.3 nm. Molecular size calculations for linezolid were carried out using ®CAChe Software (®Fujitsu Ltd.), to find out the lowest energy configuration. The calculated value was ~2.2 nm × 0.4 nm, which confirms that linezolid can be hosted inside the material mesopores.

Under the conditions used in adsorption experiments the evolution of linezolid in the liquid phase indicated that 52.3 ± 4.1% of the total linezolid present in the solution was adsorbed in the MCM-48 particles, giving a load of 9.5 ± 0.1 wt.% of linezolid in the mesoporous material. These results agree with the TGA quantification,

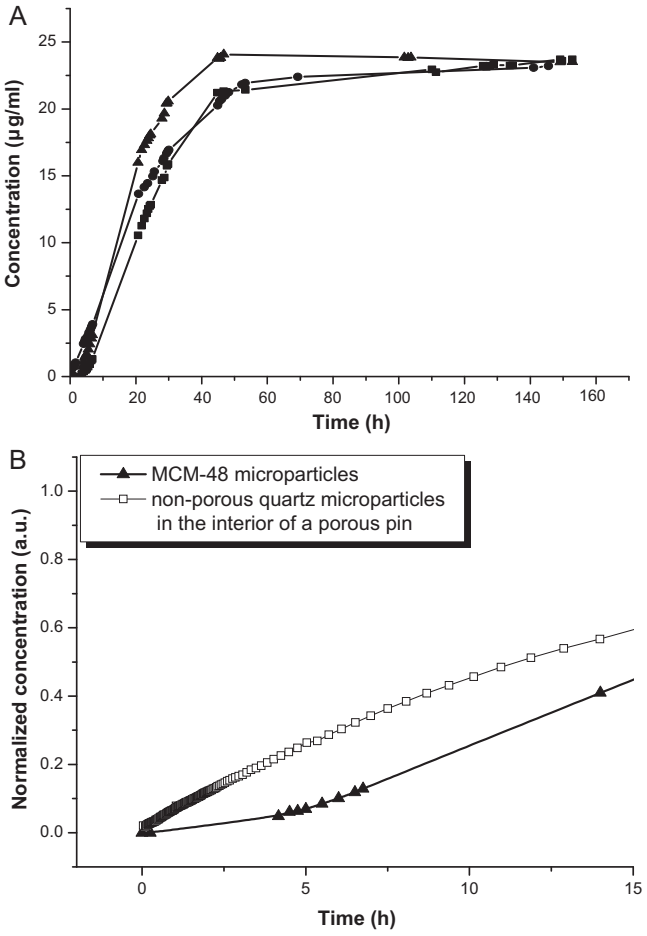

Fig. 3. (A) Linezolid release profiles in three different experiments when porous metallic pins loaded with linezolid-containing MCM-48 particles were immersed in SBF at 37 °C. (B) Normalized linezolid concentrations in the surrounding fluid obtained with porous metallic pins containing antibiotic-adsorbed MCM-48 particles and non-porous quartz microparticles of the same size with linezolid occupying inter-particle spaces.

which showed that approximately 50% of the total linezolid in solution was present as adsorbed material on the particles. TGA results showed that linezolid was burnt out at 220 °C and that weight loss was used to evaluate the amount of linezolid loaded in the mesoporous material.

Fig. 3A shows the drug release profiles obtained with 3 different pins containing MCM-48 particles loaded with linezolid. The porous pins with the microparticles were immersed in 50 mL of SBF at 37 °C and the linezolid concentration was recorded at different times. Since the total amount of microparticles loaded in the pins was approximately 37 mg, and the load of linezolid in the MCM-48 particles was 9.5 wt.% the maximum concentration attainable would be 70.3 μg/mL; however, the release reached a plateau at a concentration of ~23 μg/mL, well below the maximum concentration attainable and even farther from the solubility limit (~3 mg/mL, Curtin et al., 2003). This indicates that the concentration of the antibiotic in the limited solution volume (50 mL) and the concentration of the antibiotic still adsorbed on the mesopores have reached dynamic equilibrium, which in this case occurs when over half of the drug is still adsorbed in the mesopores. However, in a real application (e.g. an antibiotic-releasing prosthesis) a continuous renovation of the fluid surrounding the implant would take place leading to further drug release.

Without considering the initial lag-time the release profiles follow a typical first-order release. This lag-time is always present when desorbing from porous materials, but in this case it is enhanced because of the two serial mass transfer resistances introduced in the system. Initially, the SBF will enter the reservoir through the porous metal wall, filling the voids between the microparticles of the inner mesoporous bed. The drug then diffuses into the fluid filling the reservoir, where its concentration increases. The driving force for permeation builds up as the linezolid concentration inside the reservoir increases and therefore permeation through the porous reservoir wall starts to occur, slowly at first, then faster, then more slowly again as the concentration outside the reservoir increases. The differences between the release profiles obtained with the 3 pins tested are small, and might be attributed to the slight differences in the amount of drug loaded in the particles, in the packing density of the microparticles (which would give rise to a different bed porosity and degree of agglomeration, and therefore to different diffusion paths) and in the permeability of the porous wall produced during the manufacturing of the sintered stainless steel pins.

In a separate experiment a hollow pin was loaded with quartz microparticles of a similar size to the silica particles used in Fig. 3A, and the bed voidage (inter-particle voids) was filled with linezolid solution (2 mg/mL). The release behavior can be compared to the case just shown, when linezolid is not only present in the interstitial fluid but also adsorbed in the pores of the particles that constitute the inner packed bed (one of the experiments in Fig. 3A is also shown for comparison in Fig. 3B). A strong contrast can be observed between the release profiles in both cases. When the porous pin is packed with non-porous quartz particles there is virtually no drug adsorbed, and a much faster release can be observed. In spite of this, the drug concentration in the fluid outside the pin increases progressively, which is a consequence of the mass transport resistance introduced by the porous pin wall, as could be expected from its characteristics: low nominal filtration cut-off size (200 nm), inherent tortuosity, low porosity (17%) and considerable wall thickness (1.6 mm). The rate of diffusion through the porous wall could be further decreased by reducing the pore size of the reservoir wall, by increasing the wall thickness or by decreasing the permeation area of the device. Since the same porous wall is present in both experiments in Fig. 3B, the difference between both curves shows the effect of the first stage of the mass transfer process (desorption of the drug in the reservoir inner space) on the overall drug release behavior.

The experiments in Fig. 3 shows that a concentration plateau is reached when the concentration in the surrounding SBF increases sufficiently, thus limiting the amount of drug released. However as already mentioned in a real application (e.g. an antibiotic-releasing prosthesis) a continuous renovation of the fluid surrounding the implant would take place and additional drug release can be expected. This was tested by renewing the surrounding at periodic intervals. Fig. 4 shows that SBF renewal was effective in promoting further drug release, and in fact almost all of the linezolid adsorbed in the mesoporous silica could be desorbed with a single renovation.

3.2. Bactericidal studies

The MIC and MBC for the linezolid were calculated separately and values of 2 and 16 μg/mL, respectively were obtained which agrees with the values previously reported by other authors (Giacometti et al., 2005; LaPlante et al., 2008; Onda et al., 2001).

The linezolid-loaded pins showed a clear bactericidal effect up the maximum period tested (48 h, Fig. 5). When a pin loaded with mesoporous silica but without linezolid adsorbed on its mesopores was used as control a linear growth of bacteria was observed. The bacterial growth for this control was 5.65×10^7 CFU/mL after 48 h. However, for the two pins loaded with linezolid-loaded meso-

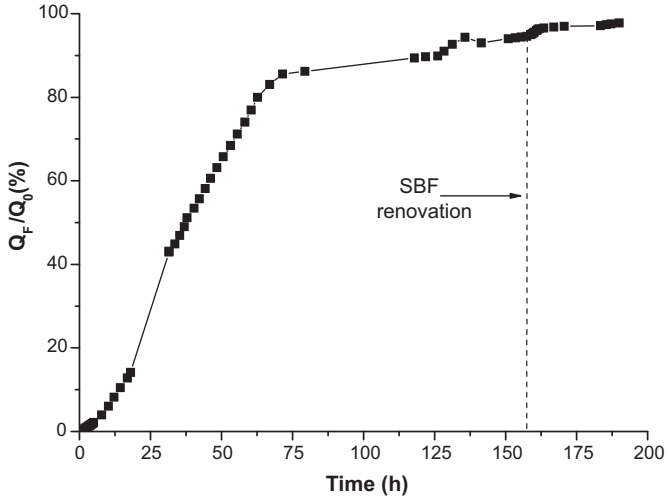

Fig. 4. Linezolid released (Q_F) as a percentage of the linezolid loaded initially (Q_0) in the mesoporous silica. Release profile obtained with a single renovation of the immersion media. It is important to point out that in this case, by carrying out a renovation, the immersing volume used was 100 mL instead of 50 mL.

porous silica, the bacterial growth leveled out or even decreased reaching a value as low as 1.31×10^4 CFU/mL. This is an excellent result taking into account that it is applied to biofilms, where killing bacteria may require up to 1000 times the antibiotic dose necessary to achieve the same result in a suspension of bacteria (Smith, 2005). In this case the maximum dose achieved from the loaded pins under the conditions used was ~54 times higher than the MBC and with that dose the bacterial growth was kept steady inhibiting their proliferation. Therefore, the drug-loaded pins effectively controlled the bacterial growth up to 3 orders of magnitude after 48 h. The bactericidal effect was also corroborated by direct observation of bacterial growth on the porous pins used. Fig. 6A shows the general appearance of the culture medium with the drug-releasing pin. A clear difference in terms of turbidity (caused by bacterial growth) is evident between linezolid-eluting pins (right) and the control experiments where microparticles without antibiotic were loaded inside the pins. Bacterial colonies were also directly observed using electron microscopy. Fig. 6B and C shows the differences in terms of bacterial adhesion on surface of the porous pins when they were loaded with the silica particles containing linezolid adsorbed on its mesopores. In 24 h large bacterial clusters are clearly observed

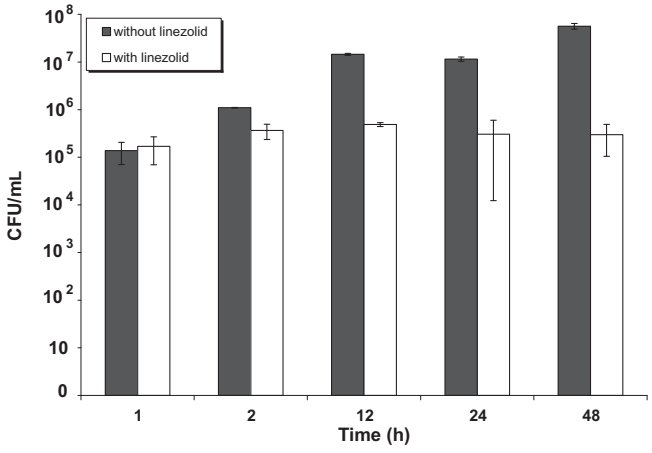

Fig. 5. Bactericidal effect of pins loaded with mesoporous silica. For the pin labeled as "with linezolid" the material had linezolid adsorbed in the mesopores while the labeled as "without linezolid" contained only the MCM-48 particles. For each contact time duplicate experiments were carried out.

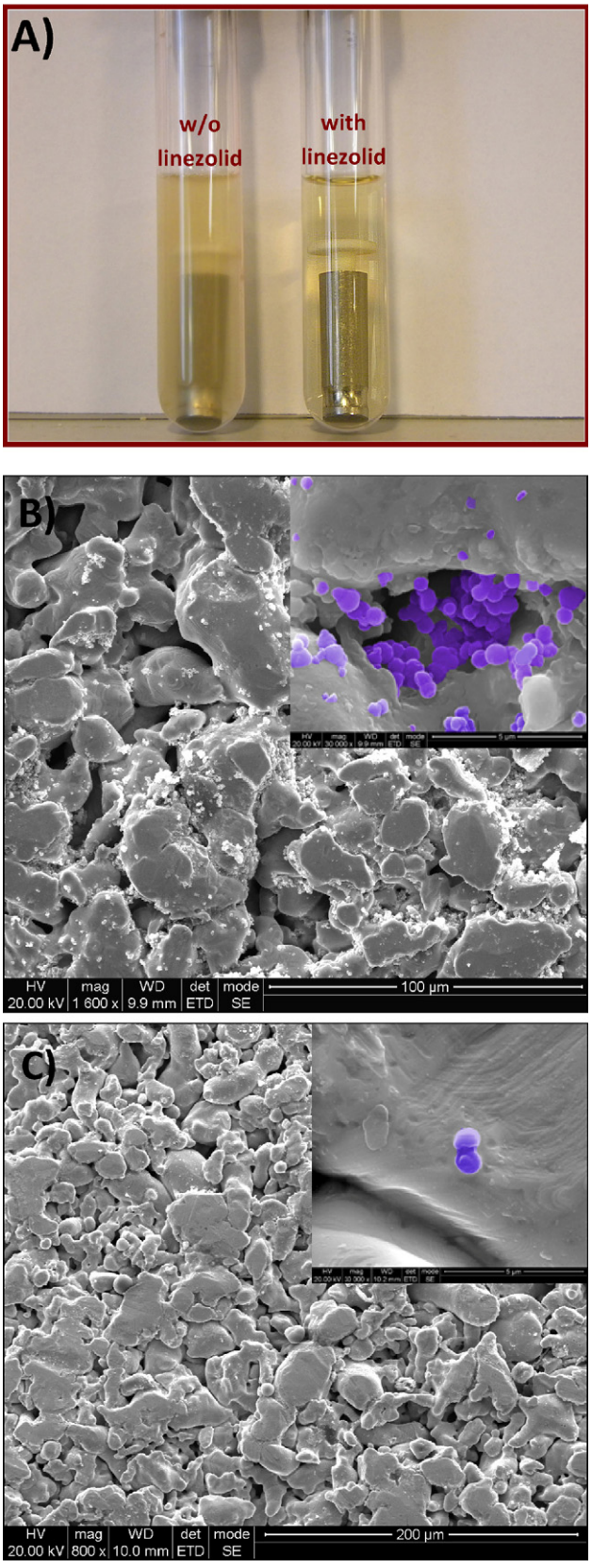

Fig. 6. Bacterial colonization on the wall of stainless steel porous pins after 24 h of incubation with *Staphylococcus aureus*. (A) Pins containing MCM-48 with linezolid adsorbed (right) and without linezolid (left) after 24 h culturing with SA. (B) SEM photographs of pins containing MCM-48 particles and (C) pins containing MCM-48 particles with linezolid adsorbed in their pores. Insets: representative bacteria (computer colored) of each sample.

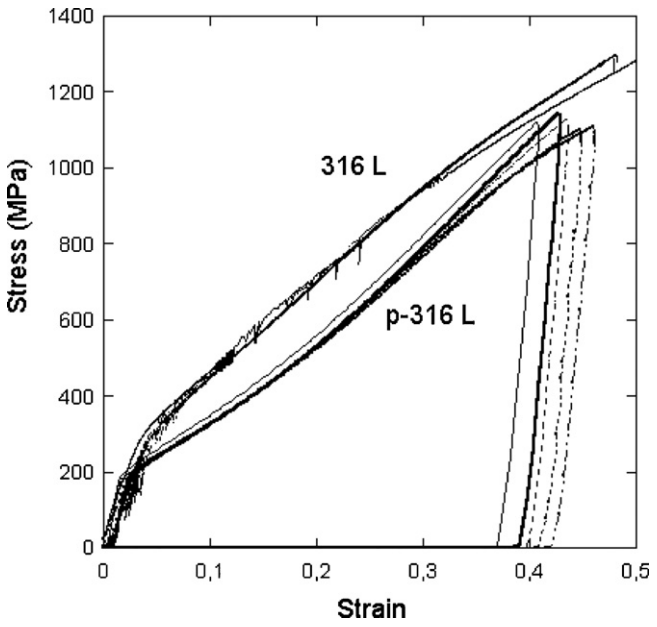

Fig. 7. Stress–strain compression curves for the porous (p-316L) and solid stainless steel 316L tubing.

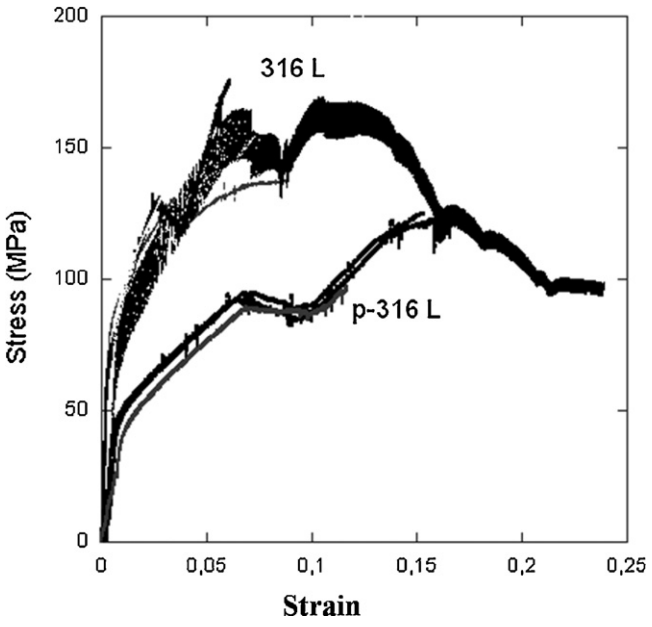

Fig. 8. Bending test results for the porous and compact stainless steel tested.

in the absence of linezolid (Fig. 6B) but when linezolid-loaded silica particles were used as filling in the hollow interior of the pins bacteria showed up only sparsely (Fig. 6C).

3.3. Mechanical studies

If hollow porous stainless steel pins are contemplated for potential use as drug-eluting structural material, they must be able to withstand the mechanical stresses involved in their utilization. To test this, a battery of mechanical tests was performed. The stress–strain, σ–ε, curves of the compression test for the porous and solid samples are plotted in Fig. 7. Similar qualitative behavior appears in both materials. The first part of the curve shows a linear trend, characterized by an elastic modulus, E, which is practically the same in both materials. This linear region finishes at the compression yield stress σy, but with main differences in both materials. So, the 316L starts the plastic regimen at approximately 300 MPa, whereas, the porous metal reaches this point at lower stresses, around 200 MPa. The following step corresponds to a large deformation associated to the plastic flow showing a lower slope. This plastic behavior can be observed by the permanent strain which appears after the unload curve, which slope is similar to the initial slope as it was expected. The test is stopped at strains close to 0.5 without reaching fracture. Literature associated with the mechanical properties of cortical bone estimated values for the ultimate strength of human cortical bone in compression close to 200 MPa (Elices, 2000). Therefore, although the pores present in the porous steel introduce a loss of the stiffness in compression mode compared to the solid material, which can be evaluated in a 50% less, the porous steel tested shows mechanical properties similar to the cortical bone.

Bending tests were carried out with both porous and solid tubes. When a sample is loaded in bending, tensile stresses are generated at the convex surfaces and compression stresses are generated at the concave surfaces. In order to compare the bending results of both materials, which were carried out on samples with different dimensions, we have plotted in Fig. 8 instead of the load–deformation, F–δ, curves showing the maximum tensile stress versus the strain, σ–ε, using beam bending theory and assuming a linear behavior. So, $\sigma = FLR/8I$, where F is the applied load, L is the active length and I is the area moment of inertia for the hollow circular cross-section, which is given by the relation: $I = \pi(R_{ext}^4 - R_{int}^4)/4$. The strain is calculated from the deformation by the expression: $\varepsilon = \delta 6D/2L$. The slope of the initial straight line portion of the stress–strain diagram is the Young's modulus, E. The bending test, at difference of the compression test, is sensitive to the influence of the porosity on the stiffness. The initial slope in the porous material is lower than in the solid material, according to the McElhaney–Byars expression $E = Eo(1 - bp + cp^2)$, where p is the porosity, Eo the elastic modulus for the compact material and b and c are fitting parameters.

The results show that the porous stainless steel pins used in this work reached values of 130 MPa. This is considerably smaller than the ultimate stress obtained for solid tubing, rated at 584 MPa (Cigada et al., 1993). However, this value seems high enough to withstand the mechanical stress during healing of a bone fracture. Indeed, the value of 130 MPa is not far from the ultimate tensile stress supported by the long human bones, which was rated by Reilly and Burstein (1975) as 176 MPa.

Finally, from the torsion test results, the values of the maximum torque, T_{max}, for the porous and the solid steels were 40.46 ± 0.61 Nm and 100.77 ± 1.90 Nm, respectively. According with the expression $\tau_{max} = T_{max}\ R_{ext}/I$, the calculated shear strengths τ_{max} were 1651 MPa and 1180 MPa. In both cases, the ultimate strength is higher than the values given for femoral cortical bone by Reilly and Burstein (1975).

4. Discussion

To our knowledge, this is the first time that the interior of pins is loaded with a drug-eluting mesoporous material using porous walls as barriers for the drug diffusion. Other works have used the empty space of hollow implants to add medical functionality. Thus, Graichen et al. (1999, 2007) loaded microelectronic-telemetry systems to measure *in vivo* the joint loads in shoulder and hip endoprosthesis, and Martin et al. (2005) loaded proteins and dyes. Unlike these works, here the inner space is not filled directly with the drug, but with the drug adsorbed in a porous material.

In spite of the complexity introduced by the dual-stage release process used here, the release profile seems to be fairly repro-

ducible. As already noted, for the three independent experiments of Fig. 3, it is likely that differences exist regarding the drug load in the silica microparticles, the packing and tortuosity of the particle bed, and the permeation characteristics (pore size, thickness) of the porous wall. Especially the porosity and tortuosity in the packed bed is a variable that depends on the particle size distribution and on the ratio between particle and reservoir diameters, and is not easy to control. In spite of this, the packing method used and the relatively uniform particle size distribution provided good reproducibility and only small differences were observed in the linezolid release profiles. Additional optimization and standardization of loading procedures should reduce these differences even further.

With the design described here the drug-loaded pins effectively reduced the bacterial growth by 3 orders of magnitude after 48 h. A complete eradication of the bacteria was not achieved due to biofilm formation. However, this limitation can be overcome by increasing the amount of linezolid released, e.g. by considering multiple pins in real applications, by designing pins with larger dimensions (larger permeation area and larger inner loading volume). Also, the amount of linezolid loaded in the mesoporous material is expected to be much higher when only the active ingredient is used for loading. In our work however, in addition to linezolid other components such as glucose monohydrate, sodium citrate, citric acid anhydrous, and hydrochloric acid that constitute the pharmaceutical formulation were present in the solution used for adsorption. Since multicomponent adsorption is a competitive process, the presence of other components reduced the useful payload of the mesoporous silica.

The approach described in this work is also different from that of Sudo et al. (2008) who loaded the inside of ceramic blocks with a powdered antibiotic (the dose of antibiotics in each ceramic block ranged from 100 to 400 mg) and they successfully implanted them in 7 patients without recurrent infection in 6 of them. The concept proposed here is different in the sense that it couples two stages in which the mass transfer rate can be independently tailored by adjusting the characteristics of the microparticles and of the porous wall. The application envisioned here targets temporary fixation systems that will be removed when the fracture heals. This helps to avoid inducing bacterial linezolid resistance by the residual antibiotic that might occur if a ceramic integrable implant was used. A similar case of resistance has been described for gentamicin-loaded polymethylmethacrylate beads (Neut et al., 2003). In addition, the amount of drug can be determined by the inner volume of the hollow implant, which presents obvious advantages in terms of the useful payload achievable compared to antibacterial coatings on implants (e.g. gentamicin-PDLLA-coated tibia nails, UTN Synthes® GmbH, Umkirch, Germany) where the amount of drug is more limited.

This work presents only the device concept and some preliminary results. Optimization of drug release rates will be the subject of future works, where the effect of the two sets of material characteristics respectively related to the microparticles (pore structure, packing density, size) and to the reservoir (pore diameter, wall thickness, permeation area per unit volume) will be investigated. Future developments should also consider the many different possibilities of mesoporous silicas in terms of pore size, particle size and surface functionalization, as well as the possibility of defining different spaces within the reservoir to encapsulate different drugs, each with an optimized release rate. Finally, the possibility of filling the inner of hollow porous implants with drug-releasing porous inorganic packed beds opens up new possibilities in other fields where hollow screws have been used such as maxillofacial implants (Buser et al., 1991; Cehreli et al., 2006), always with the objective of attaining a drug concentration above the MIC to avoid bacterial resistance.

5. Conclusions

A drug-eluting porous implant has been developed, consisting of a packed bed of porous microspheres inside a porous wall reservoir. Such a system has the potential for a fine control of the rate of drug release, since the variables related to the mesoporous nanoparticles and to the porous wall reservoir can be manipulated independently. The concept was tested in an antibiotic releasing scenario, where the reproducibility of drug release patterns was demonstrated. The mechanical resistance of the porous steel proposed as a drug-eluting implantable pin was tested in uniaxial and unconfined compression tests, three point bending tests, and torsion tests and found sufficient for clinical use. Drug eluting experiments in which nonporous particles were packed inside the reservoir showed a marked different release profile, showing the influence of drug adsorption in the microparticles on the overall release process.

Conflict of interest

None declared.

Acknowledgments

This work was supported by grant MEC CICYT, SAF2008-03446 from the *Ministerio de Educación y Ciencia* (Spain). M.A. acknowledges the support from the 2006 *Ramón y Cajal* program (order ECI/158/2005) and the *Fundación Ramón Areces*. We thank Dr. I. Lasa, Institute of Agrobiotechnology (Pamplona, Spain) for kindly supply of the bacterial strain and Jesús Peñaranda for providing valuable assistance in the laboratory.

References

Arruebo, M., Vilaboa, N., Santamaria, J., 2010. Drug delivery from internally implanted biomedical devices used in traumatology and in orthopedic surgery. Expert Opin. Drug Deliv. 7, 1–15.

Bernard, L., Hoffmeyer, P., Assal, M., Vaudaux, P., Schrenzel, J., Lew, D., 2004. Trends in the treatment of orthopaedic prosthetic infections. J. Antimicrob. Chemother. 53, 127–129.

Bibbo, C., Brueggeman, J., 2010. Prevention and management of complications arising from external fixation pin sites. J. Foot Ankle Surg. 49, 87–92.

Buchholz, H.W., Engelbrecht, H., 1970. Depot effects of various antibiotics mixed with Palacos® resins. Chirurg 41, 511–515.

Buser, D., Weber, H.P., Bragger, U., Balsiger, C., 1991. Tissue integration of one-stage ITI implants: 3-year results of a longitudinal study with hollow-cylinder and hollow-screw implants. Int. J. Oral Maxillofac. Implants 6, 405–412.

Cehreli, M., Akkocaoglu, M., Akca, K., 2006. Numerical simulation of *in vivo* intraosseous torsional failure of a hollow-screw oral implant. Head Face Med. 2, 36–43.

Cigada, A., De Soutis, G., Gratti, A.M., Roos, A., Zaffe, D.J., 1993. In vivo behavior of a high performance duplex stainless steel. J. Appl. Biomater. 4, 39–46.

Clark, P.A., Moioli, E.K., Sumner, D.R., Mao, J.J., 2008. Porous implants as drug delivery vehicles to augment host tissue integration. FASEB J. 22, 1684–1693.

Curtin, J., Cormican, M., Fleming, G., Keelehan, J., Colleran, E., 2003. Linezolid compared with eperezolid, vancomycin, and gentamicin in an in vitro model of antimicrobial lock therapy for *Staphylococcus epidermidis* central venous catheter-related biofilm infections. Antimicrob. Agents Chemother. 47, 3145–3148.

Elices, M., 2000. Structural Biological Materials, Design and Structure–Property Relationships. Ed. Pergamon Pergamon Materials Series, Oxford, UK.

Engesaeter, L.B., Lie, S.A., Espehaug, B., Furnes, O., Vollset, S.E., Havelin, L.I., 2003. Antibiotic prophylaxis in total hip arthroplasty: effects of antibiotic prophylaxis systemically and in bone cement on the revision rate of 22,170 primary hip replacements followed 0–14 years in the Norwegian Arthroplasty Register. Acta Orthop. Scand. 74, 644–651.

Giacometti, A., Cirioni, O., Ghiselli, R., Orlando, F., Mocchegiani, F., Silvestri, C., Licci, A., De Fusco, M., Provinciali, M., Saba, V., Scalise, G., 2005. Comparative efficacies of quinupristin-dalfopristin, linezolid, vancomycin, and ciprofloxacin in treatment, using the antibiotic-lock technique, of experimental catheter-related infection due to *Staphylococcus aureus*. Antimicrob. Agents Chemother. 49, 4042–4045.

Graichen, F., Bergmann, G., Rohlmann, A., 1999. Hip endoprosthesis for *in vivo* measurement of joint force and temperature. J. Biomech. 32, 1113–1117.

Graichen, F., Arnold, R., Rohlmann, A., Bergmann, G., 2007. Implantable 9-channel telemetry system for *in vivo* load measurements with orthopedic implants. IEEE Trans. Biomed. Eng. 54, 253–261.

Kokubo, T., Kushitani, H., Sakka, S., 1990. Solutions able to reproduce *in vivo* surface-structure changes in bioactive glass–ceramic A-W3. J. Biomed. Mater. Res. 24, 721–734.

LaPlante, M.K.L., Leonard, S.N., Andes, D.R., Craig, W.A., Rybak, M.J., 2008. Activities of clindamycin, daptomycin, doxycycline, linezolid, trimethoprim-sulfamethoxazole, and vancomycin against community-associated methicillin-resistant *Staphylococcus aureus* with inducible clindamycin resistance in murine thigh infection and *in vitro* pharmacodynamic. Antimicrob. Agents Chemother. 52, 2156–2162.

Laurent, F., Bignon, A., Goldnadel, J., Chevalier, J., Fantozzi, G., Viguier, E., Roger, T., Boivin, G., Hartmann, D., 2008. A new concept of gentamicin loaded HAP/TCP bone substitute for prophylactic action: *in vitro* release validation. J. Mater. Sci.: Mater. Med. 19, 947–951.

Lew, D.P., Waldvogel, F.A., 2004. Osteomyelitis. Lancet 364, 369–379.

Martin, F., Walczak, R., Boiarski, A., Cohen, M., West, T., Cosentino, C., Ferrari, M., 2005. Tailoring width of microfabricated nanochannels to solute size can be used to control diffusion kinetics. J. Control. Release 102, 123–133.

Mason, W.T.M., Khan, S.N., James, C.L., Chesser, T.J.S., Ward, A.J., 2005. Complications of temporary and definitive external fixation of pelvic ring injuries. Injury 36, 599–604.

Neut, D., van de Belt, H., van Horn, J.R., van der Mei, H.C., Busscher, H.J., 2003. Residual gentamicin-release from antibiotic-loaded polymethylmethacrylate beads after 5 years of implantation. Biomaterials 24, 1829–1831.

Onda, H., Wagenlehner, F.M.E., Lehn, N., Naber, K.G., 2001. In vitro activity of linezolid against Gram-positive uropathogens of hospitalized patients with complicated urinary tract infections. Int. J. Antimicrob. Agents 18, 263–266.

Pérez, L.M., Arruebo, M., Irusta, S., Gracia-Villa, L., Santamaría, J., Puértolas, J.A., 2007. Mechanochemical characterisation of silica-based coatings on nitinol substrates. Micropor. Mesopor. Mater. 98, 292–302.

Reilly, D.T., Burstein, A.H., 1975. The elastic and ultimate properties of compact bone tissue. J. Biomech. 8, 393–405.

Smith, A.W., 2005. Biofilms and antibiotic therapy: is there a role for combating bacterial resistance by the use of novel drug delivery systems? Adv. Drug Deliv. Rev. 57, 1539–1550.

Sudo, A., Hasegawa, M., Fukuda, A., Uchida, A., 2008. Treatment of infected hip arthroplasty with antibiotic-impregnated calcium hydroxyapatite. J. Arthroplasty 23, 145–150.

Vallet-Regi, M., 2006. Revisiting ceramics for medical applications. Dalton Trans., 5211–5220.

Wikler, M.A., 2009. National Committee for Clinical Laboratory Standards. Methods for dilution antimicrobial susceptibility test for bacteria that grow aerobically. 8th edition. Approved standard M7-A8, vol. 29 (2). National Committee for Clinical Laboratory Standards, Wayne, PA, USA.

Wu, J.A., Kusuma, C., Mond, J.J., Kokai-Kun, J.F., 2003. Antimicrob. Agents Chemother. 47, 3407–3414.

Yu, D., Wong, J., Matsuda, Y., Fox, J.L., Higuchi, W.I., Otsuka, M., 1992. Self-setting hydroxyapatite cement: a novel skeletal drug delivery system for antibiotics. J. Pharm. Sci. 81, 529–531.